Available online at www.sciencedirect.com
ScienceDirect
Journal of the European Ceramic Society 29 (2009) 905–911
www.elsevier.com/locate/jeurceramsoc

Ink-jet printing of ceramic micro-pillar arrays

M. Lejeune [a,*], T. Chartier [a], C. Dossou-Yovo [b], R. Noguera [b]

[a] SPCTS-UMR 6638, 47 à 73, Avenue Albert Thomas, 87065 Limoges Cedex, France
[b] CERADROP-ESTER Technopole, BP 36921, 87069 Limoges, France

Available online 23 September 2008

Abstract

This review illustrates the fabrication of different kinds of micro-pillar array structures by ink-jet printing process. So the fabrication of 1–3 piezoelectric composites and photocatalytic devices by deposition, respectively of PZT and TiO_2 suspensions will be mainly reported. First, different investigations were carried out to adjust the ceramic suspensions to be compatible with ink-jet printing process. Afterwards, this study reveals how the main characteristics of the micro-pillar array structures (morphology, definition, compacity, etc.) strongly depend on the conditions of fabrication (configuration of the deposit, driving parameters of the printing head, delay between two successive layers, etc.) and on the formulation of the ceramic suspensions (ceramic loading, nature and content of binder and surfactant, etc.). Finally, sintered PZT and TiO_2 micro-pillar structures were achieved with a very good definition (around 40 μm). The study of the functional properties of the corresponding structures is in progress.

Keywords: Printing; Suspensions; PZT; TiO_2

1. Introduction

The ink-jet printing process has been recently explored as a solid freeforming fabrication (SFF) technique to produce 3D ceramic parts.[1–11] The prototyping techniques developed up to now for ceramic parts such as stereolithography,[12–16] fused deposition modeling[17,18] and selective laser sintering[19] are characterized by a definition of around 150 μm, and do not allow to deposit different materials on the same layer. In comparison, ink-jet printing prototyping process opens the way to the development of multifunctional 3D fine scale ceramic parts.

Ink-jet printing prototyping process consists in the deposition of ceramic system micro-droplets (a few pl) ejected via nozzles to build the successive layers of the 3D structures. By adjusting the aperture of the printing head and by controlling the spreading phenomenon of the droplet, one can expect to reach a standard definition of around 50 μm and ultimately of 10 μm, taking into account the tremendous evolution in the printing field.

In order to demonstrate the potentiality of the ink-jet printing for the fabrication of 3D fine scale ceramic parts, our investigations have been focused on the case of micro-pillar array structures for different applications such as:

- PZT skeleton, which once embedded in polymer, can be used as 1–3 piezoelectric ceramic polymer composite for medical imaging probes. The ink-jet printing process could lead to the evolution of medical imaging probes in terms of performances thanks to the improvement (i) of their spatial resolution by generating very fine ceramic structures (ii) of their configuration by variable size, shape and distribution of ceramic rods inside the probes.
- TiO_2 skeleton for photocatalytic devices. Once covered by a TiO_2 layer (anatase), the TiO_2 micro-pillar structures can be very promising for photocatalytic applications because of the exchange surface increase compared to a plane configuration.

2. Adjustment of the ceramic (PZT, TiO_2) suspensions in regards to fluid properties

For ink-jet printing, the fluids must have a viscosity and a surface tension ranging between 5 and 20 mPa s and between 30 and 35 mN/m, respectively, which correspond to the specifications given by the printing head supplier. In addition, to obtain droplet generation, a ratio of ejection $Re/We^{1/2}$ $[=(\sigma\rho r)^{1/2}/\eta]$, in the adequate range (1–10), is required to minimize pressure for ejection and avoid satellite droplet formation.

Therefore, different investigations were carried out to adjust the ceramic suspension formulation in terms of nature and content of the different organic compounds (solvent, dispersant,

* Corresponding author. Tel.: +33 5 55 45 22 27; fax: +33 5 55 79 09 98.
E-mail addresses: martine.lejeune@unilim.fr (M. Lejeune), r_noguera@ceradrop.fr (R. Noguera).

0955-2219/$ – see front matter © 2008 Elsevier Ltd. All rights reserved.
doi:10.1016/j.jeurceramsoc.2008.07.040

binder, etc.) and of the ceramic loading to be compatible with the ink-jet printing process, (i) in regards to the fluid properties mentioned previously and, (ii) to avoid sedimentation or premature drying of the ink within the nozzle, which can induce the blocking of the printing head. In fact, the blocking of the nozzle means that agglomeration of particles prevent the nozzle from ejecting droplets.

Moreover, the formulation of the ceramic suspensions was also chosen taking into account the optimal characteristics of the deposit for each layer, i.e. (i) high green compacity, (ii) large and homogeneous thickness, (iii) high definition and (iv) high green mechanical strength. These aspects will be underlined in Section 4.1.

At first, water was selected as solvent for ceramic (PZT or TiO_2) suspensions to combine a slow evaporation with environmental benefits. Moreover, for ceramic suspensions, the particle size distribution of the powder must be adjusted to obtain a ratio of 50 between the radius of the nozzle aperture and the maximum diameter of the powder to avoid the blocking of the nozzle. Consequently, as the minimum aperture of our printing heads is equal to 52 μm, the maximum diameter of the PZT and TiO_2 powders was adjusted by attrition milling to 1 μm with a mean diameter of 0.4 μm.

The content of dispersant was adjusted to reach a minimum viscosity at the end of the milling step of (PZT or TiO_2) powders corresponding to a high ceramic loading (around 40 vol.%) to guarantee the stability of the ceramic suspension in the reservoir of the ink-jet printing equipment.

After dilution, the ceramic (PZT or TiO_2) suspensions for ink-jet printing exhibit a Newtonian behavior. Fig. 1a shows the variation of the viscosity of 15 vol.% PZT-loaded suspensions as a function of the PZT/(PZT + binder) vol.%, for binders characterized by different molecular weights. This reveals that the increase of the molecular weight of the binder allows to obtain the appropriate viscosity of the suspension (i.e. 10 mPa s) for a higher PZT/(PZT + binder) vol.%, i.e., 75% (ink 2) compared to 67% (ink 1). The variation of the viscosity as a function of the PZT/(PZT + binder) vol.%, for suspensions characterized by variable PZT loading (10 or 15 vol.%) prepared with a high molecular weight binder is reported in Fig. 1b. The increase of the ceramic loading of the suspension allows to reach the appropriate value of viscosity (i.e. 10 mPa s) for a higher PZT/(PZT + binder) vol.%, i.e. 75% (ink 2) compared to 60% (ink 3). In both cases, the increase of the PZT/(PZT + binder) vol.%, could contribute to increase further the densification rate of the sintered micro-pillars.

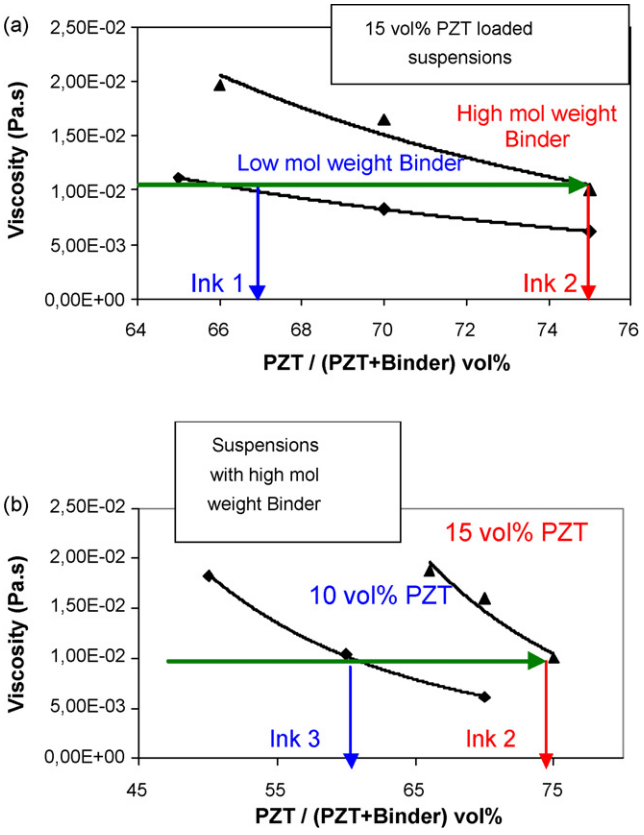

Fig. 1. Variation of the viscosity as a function of the PZT/(PZT + binder) vol.%, of (a) 15 vol.% PZT-loaded suspensions, for binders characterized by variable molecular weight (b) of suspensions characterized by variable PZT loading (10 or 15 vol.%), prepared with a high molecular weight binder.

Table 1
Fluid properties of the different inks and characteristics of the corresponding micro-pillar arrays.

Characteristics	Ink 1	Ink 2	Ink 3	Ink 4	Ink 5
Ceramic loading (vol.%)	15	15	10	10	15
Binder	Low mw[a]	High ml[a]	High ml	High ml	High ml
Surfactant	No	No	No	Yes	Yes
Ceramic/binder (vol.%)	67/33	75/25	60/40	60/40	75/25
Viscosity (mPa s)	10	10	10	10	10
Surface tension (mN/m)	59	59	59	30	30
Re/We $^{1/2}$ $[(\sigma\rho r)^{1/2}/\eta]$	7.4[b]	6.1[b]/4.3[c]	5.6[b]	3.9[c]	3.44[c]
Thickness/layer (μm)	4	10	1	3	10
$\varnothing_{\text{green pillar}}$ (μm)	75	70	71	43	50
$\varnothing_{\text{droplet}}$ (μm)	60 ± 6	60 ± 6	60 ± 6	50 ± 6	50 ± 6
Spreading factor $\varnothing_{\text{deposit}}/\varnothing_{\text{droplet}}$	1.25 ± 0.1	1.2 ± 0.1	1.2 ± 0.1	0.9 ± 0.1	1 ± 0.1
Kinetic energy (J)	–	1100×10^{-12}	950×10^{-12}	170×10^{-12}	353×10^{-12}

[a] Low mw: low molecular weight, high ml: high molecular weight.
[b] For a 60 μm nozzle aperture
[c] For a 52 μm nozzle aperture.

The three corresponding inks (1, 2 and 3—Fig. 1) were tested further to fabricate PZT micro-pillar arrays.

The three different inks are characterized by similar surface tension (around 59 mN/m). The addition of a surfactant was used to adjust the surface tension of the inks to an appropriate value of 30 mN/m. These modified inks (i.e. inks 4 and 5, respectively) were also tested for the fabrication of micro-pillar arrays.

The characteristics of the different inks are listed in Table 1.

3. Fabrication of the ceramic micro-pillar arrays

The ink-jet printing equipment was developed in the SPCTS laboratory. The main technical characteristics are as follows: the printing equipment is a drop-on-demand one[20] with multi-nozzle piezoelectric printing heads. The nozzle aperture ranges between 52 and 60 μm. The nozzles can be electrically driven (i) independently or (ii) simultaneously. The printing head displacement has a resolution of 0.5 μm, a reproducibility of 2 μm and an accuracy of 2 μm. Additional technical data are given in the corresponding patent (PCT/RF04/02150), and by the equipment manufacturer under the reference Ceraprinter L01 [Ceradrop, Ester Technopole, Porte 16, BP 36921, 87069 Limoges (France)].

Before fabrication, the electric pulse applied to the nozzle was adjusted for each ceramic suspension to have a consistent droplet ejection. This step was carried out by capturing stroboscopically backlit images of the ejection with a CCD camera. By this way, velocity and size of the droplet during ejection and before spreading were controlled as a function of the driving parameters of the printing head. Previous works[21] revealed that the final droplet velocity and volume, i.e. the droplet kinetic energy ($E_c = 2/3\rho\pi r^3 V^2$ with ρ, r, V corresponding to the density of the suspension, the droplet radius and velocity, respectively), increase with the amplitude of the pulse.

The micro-pillar arrays whose typical configuration is illustrated in Fig. 2, were obtained through successive deposition steps of droplets periodically spaced out.

As mentioned previously, to modify the delay between two successive layers, formed by displacement of the printing head in the *Y*-direction, different alternatives are possible such as, (i) to electrically drive simultaneously all the nozzles of the printing head (shortest drying time) during the displacement of the printing head or (ii) to drive only one nozzle by moving the printing head in the *X*-direction to generate successively the different droplet lines and then to come back to deposit droplets on the first level (longest drying time). The effect of the delay between the successive layers on the characteristics of the micro-pillar arrays was studied.

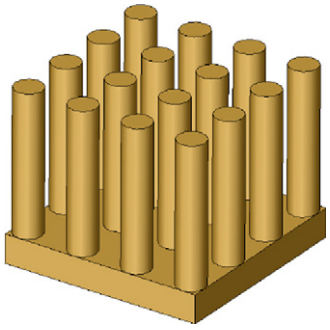

Fig. 2. Configuration of a micro-pillar array structure.

The PZT and TiO_2 micro-pillar arrays were deposited on green sheets obtained by tape casting of organic PZT or TiO_2 suspensions.

4. Characteristics of the ceramic micro-pillar arrays

4.1. Adjustment of the characteristics of PZT and TiO_2 green micro-pillar arrays

PZT micro-pillar array structures were first fabricated by electrically driving one single nozzle of the printing head (60 μm aperture) and by using the 1, 2 and 3 inks characterized by the same viscosity (10 mPa s) and surface tension (59 mN/m) but by variable molecular weight of binder (inks 1 and 2) or ceramic loading (inks 2 and 3). Whereas the droplet kinetic energy is similar in the three cases, one can observe a very good stacking of the successive layers for the ink 2 compared to the inks 1 and 3, for which there is a flowing of the suspension along the pillars during the fabrication (Fig. 3). This reveals that the fastest drying is obtained for ink 2, corresponding to the highest ceramic loading associated to a minimum quantity of the highest molecular weight of binder. This corresponds correlatively to a variation of the growth rate of the structure for a similar mean diameter of the green pillar (around 70 μm). The average deposited thickness/layer is, respectively 1 μm/layer for ink 3, 4 μm/layer for ink 1 and 10 μm/layer for ink 2. Therefore, the maximum growth rate corresponds to the highest ceramic loading associated to a minimum quantity of the highest molecular weight of the binder. The compacity of the best stacked green structure (Fig. 3b) has been evaluated to 59%, which corresponds to a total porosity of the burned structure of 56 vol.%.

In a second step, to improve the definition of the structures and to decrease the fabrication time of large micro-pillar arrays (only 4 s between two successive layers), a multi-nozzle printing head with a 52 μm aperture was used by electrically driving simultaneously different nozzles during the displacement of the printing head. In this case, the drying time between two successive layers has to be adjusted to eliminate well the solvent: in fact, too short drying times can lead to the coalescence of neighboring droplets and formation of defects such as bridges illustrated by Fig. 4. This adjustment can be performed for example through the displacement velocity of the printing head, the number of nozzles which are simultaneously electrically driven, or the space between two neighboring droplets on the same line, etc.

By this way, one can observe that a few nozzles were blocked during fabrication of PZT micro-pillar arrays with ink 2.

As the ratio of ejection remains in the good range to guarantee a correct ejection, i.e. 4.3 against 6.1 for a 60 μm aperture nozzle, the blocking of the small size nozzles (52 μm diameter) is firstly attributed to premature drying of the suspension. Therefore, the ink 3, characterized by a lower ceramic loading was selected for the further investigations to limit the blocking

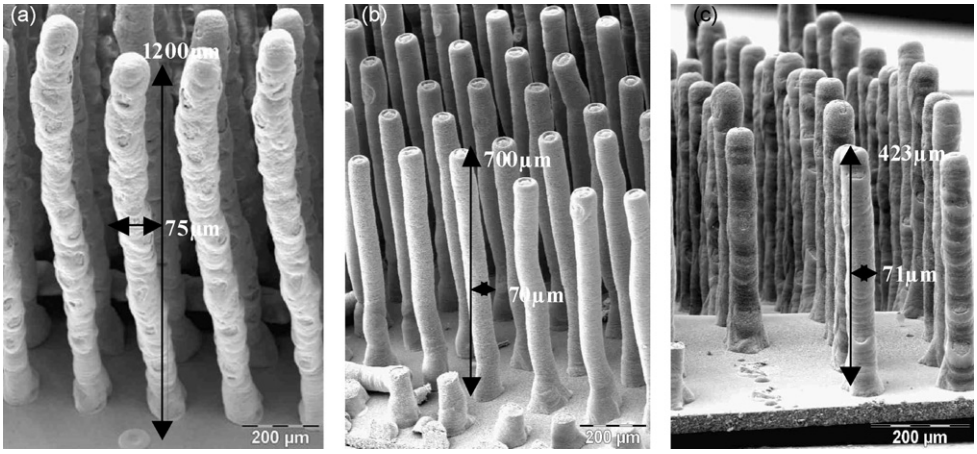

Fig. 3. Scanning electronic image of green PZT micro-pillar arrays fabricated on PZT green tape by electrically driving one single nozzle of the printing head (60 μm aperture) with (a) the ink 1 (15 vol.% PZT loading, low molecular weight binder, ceramic/binder ratio: 67/33) (b) the ink 2 (15 vol.% PZT loading, high molecular weight binder, ceramic/binder ratio: 75/25) (c) the ink 3 (10 vol.% PZT loading, high molecular weight binder, ceramic/binder ratio: 60/40).

of the nozzle. However, the ink 3 was improved because its low drying rate leads to a bad stacking of the layers as mentioned previously (Fig. 3c). Addition of a surfactant to the ink 3 (i.e. ink 4) allows to improve in this case, the stacking of the successive layers (Fig. 5). This can be explained by the positive effect of the surfactant, i.e. of the decrease of the surface tension, on the homogeneization of the deposited layer thickness and consequently on the drying of the layer.

The corresponding growth rate is equal to 3 μm/layer. The mean diameter of the pillar obtained with ink 4 ejected with a 52 μm nozzle aperture is much smaller compared to ink 3 ejected with a 60 μm nozzle aperture, i.e. 43 μm against 71 μm, respectively. Obviously, this difference of definition results partly from the lower nozzle aperture, but the slight skrinkage after droplet impact obtained with ink 4 (0.9 ± 0.1), compared to the spreading observed with ink 3 (1.2 ± 0.1) could result from the difference of the droplet kinetic energy.

For ink 4 ejected with a 52 μm nozzle aperture, the kinetic energy is very low, i.e. 170×10^{-12} J compared to 950×10^{-12} J for ink 3 ejected with the 60 μm nozzle aperture. This could mean that for ink 4 ejected with a 52 μm nozzle aperture, the spreading of the droplet is not significant, because of the very low kinetic energy and during drying, the particles could coalesce in an interaction that induces a slight skrinkage of the dried deposit.

Moreover, Fig. 6 reveals a very smooth surface at the top of the pillar obtained by ejection of the ink 4 with a 52 μm nozzle aperture compared to the one obtained with ink 2 ejected with a 60 μm nozzle aperture, which shows a segregation of powder on the edge of the pillar top. This difference could result from the combined effect of the strong decrease of the droplet energy, respectively from 1100×10^{-12} J for ink 2 to 170×10^{-12} J for ink 4, and of the modification of the formulation of the suspension, i.e. decrease of the PZT ceramic loading and addition of a

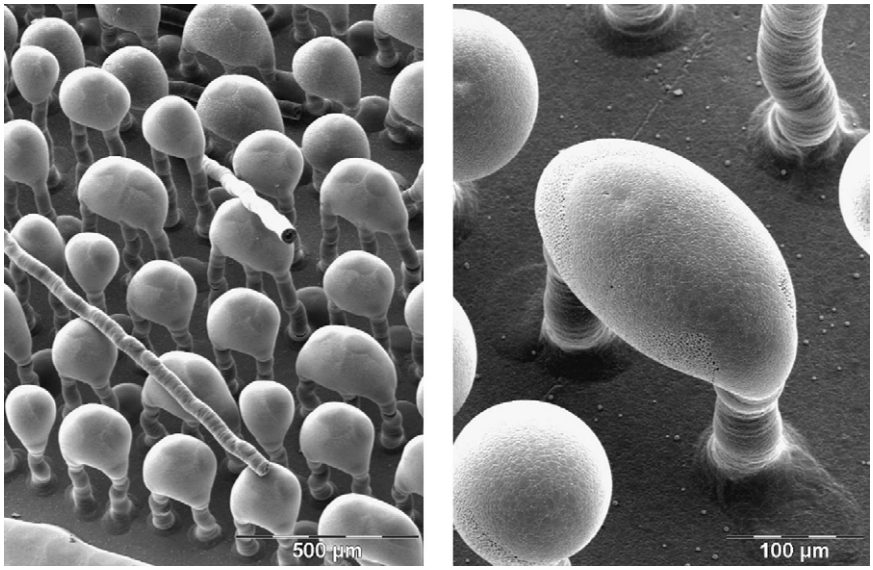

Fig. 4. Scanning electronic image of a TiO_2 micro-pillar array deposited on TiO_2 green tape by simultaneously ejection of the different nozzles of the printing head (52 μm aperture), without drying between successive layers and with a space of 200 μm between two neighboring droplets on the same line.

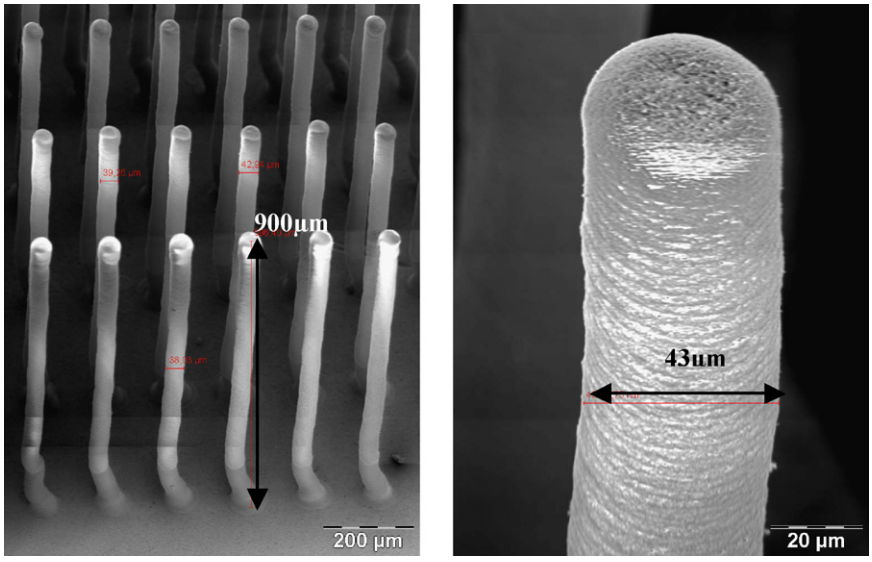

Fig. 5. Scanning electronic images of a green PZT micro-pillar array fabricated on PZT green tape by simultaneously electrically driving different nozzles of the printing head (52 µm aperture) with the ink 4 (10 vol.% PZT loading, high molecular weight binder, ceramic/binder ratio: 60/40, surfactant).

surfactant, which both contribute to increase the uniformity of the layer thickness.

Finally, to increase the growth rate, a new ink was tested (ink 5) corresponding to an increase of the PZT ceramic loading (15 vol.%) compared to ink 4 (10 vol.%), i.e. to the addition of a surfactant to ink 2. The ejection was not successful: as inks 4 and 5 exhibit the same viscosity (10 mPa s) and surface tension (30 mN/m), and a similar ratio of ejection (3.9 against 4.2, respectively), the bad ejection observed with ink 5 with a 52 µm aperture multi-nozzle printing head could result from its high density. In fact, as the density of the suspension increases from 1.7 (ink 4) to 2 (ink 5), the sound velocity in the corresponding fluids decreases correlatively, so that no ejection was possible for ink 5, whatever the type of pulse applied to the 52 µm aperture multi-nozzle printing head.

For the fabrication of large TiO_2 micro-pillar arrays with a 52 µm aperture multi-nozzle printing head, the last results obtained for PZT structures were taken into account: one can expect to eject ink 5 (15 vol.% TiO_2) with a 52 µm aperture multi-nozzle printing head as the ejection of ink 4 (10 vol.% PZT) with the same device was successful. In fact, both have the same viscosity, surface tension and ratio of ejection. Moreover, a 15 vol.% TiO_2-loaded suspension has a density very close to the one of a 10 vol.% PZT-loaded suspension, i.e. 1.5 and 1.7, respectively. Consequently the sound velocity in the two fluids is similar. The large TiO_2 micro-pillar array fabricated with ink 5 exhibits a growth rate similar to ink 2 (i.e. 10 µm/layer) which corresponds to a high green compacity of 64% and therefore a total porosity of the burned structure equal to 52 vol.%. As for PZT structures obtained with ink 4, the TiO_2 structures using ink

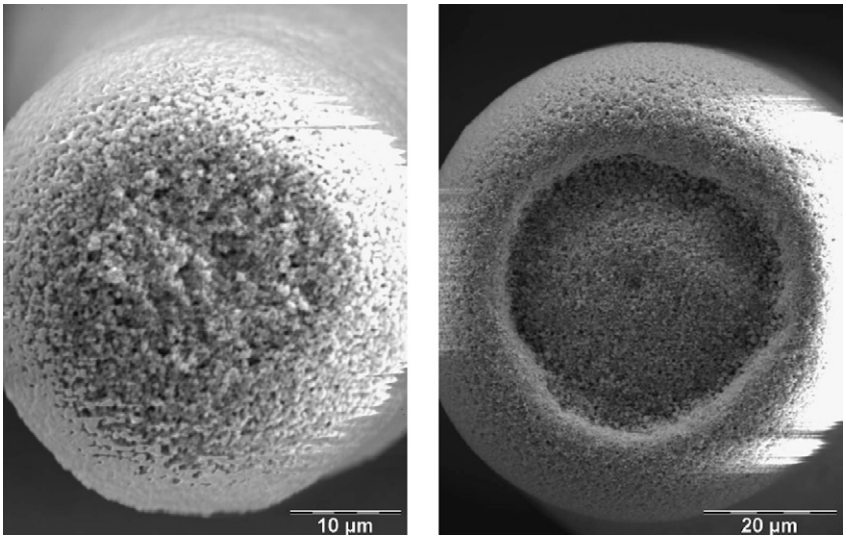

Fig. 6. Top of pillars obtained by ejection of (a) the ink 4 with a 52 µm nozzle aperture ($E_c = 170 \times 10^{-12}$ J) (b) the ink 2 ejected with a 60 µm nozzle aperture ($E_c = 1100 \times 10^{-12}$ J).

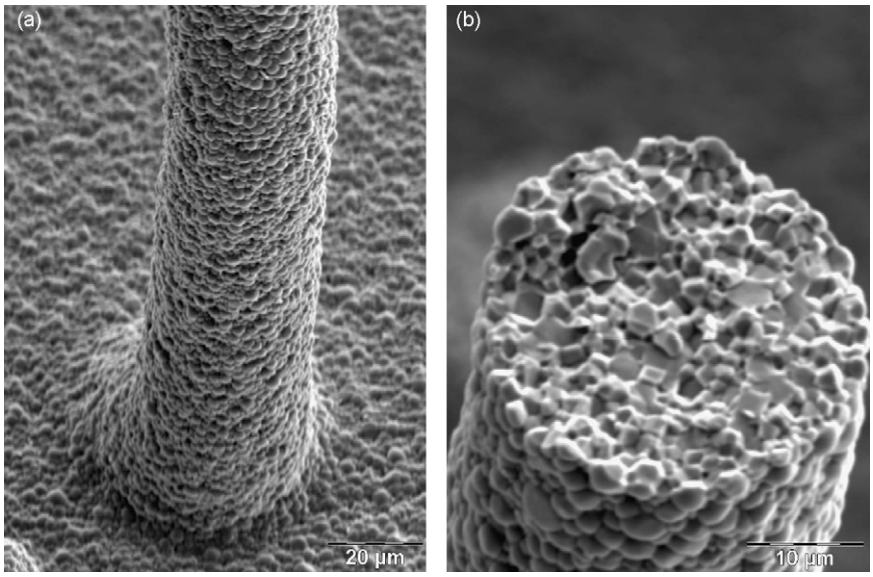

Fig. 7. Scanning electronic images of (a) a sintered PZT micro-pillar and (b) of its cross-section, fabricated on PZT green tape by simultaneously electrically driving different nozzles of the printing head (52 μm aperture) with the ink 4 (10 vol.% PZT loading, high molecular weight binder, ceramic/binder ratio: 60/40, surfactant).

5 exhibit a high definition (50 μm pillar diameter) corresponding to a spreading factor of 1 ± 0.1. The low spreading factor could be partly explained (as for PZT structures using ink 4), by the low corresponding droplet kinetic energy (353×10^{-12} J).

4.2. Sintering of PZT and TiO_2 micro-pillar arrays

Once the conditions of fabrication of large PZT or TiO_2 micro-pillar arrays were optimized as previously shown in Section 4.1, different trials were performed to adjust the sintering conditions.

For the large PZT micro-pillar arrays fabricated with a 52 μm aperture multi-nozzle printing head (ink 4), a specific PbO sintering atmosphere was used to guarantee the stoechiometry of the sintered material, taking into account the high corresponding exchange surface of the structure. After sintering at 1250 °C, very dense pillars were obtained characterized by a mean diameter of 34 μm (Fig. 7), which corresponds to a shrinkage of 21%.

The sintered PZT skeleton was then embedded in a polymer matrix and the thickness of the composite was adjusted to a value around 300 μm to avoid lamb waves resonance. This structure is very promising because of the very low pillar diameter: one can expect to develop very high frequency transducers and consequently to improve the spatial resolution of the ultrasonic probes. Piezoelectric characterization of these structures is in progress.

On the other side, large TiO_2 micro-pillar arrays fabricated with a 52 μm aperture multi-nozzle printing head (ink 5) were sintered at 1300 °C. Highly dense pillars with a diameter of 40 μm are obtained which corresponds to a shrinkage of 20% (Fig. 8). A good adhesion on the substrate is observed which is

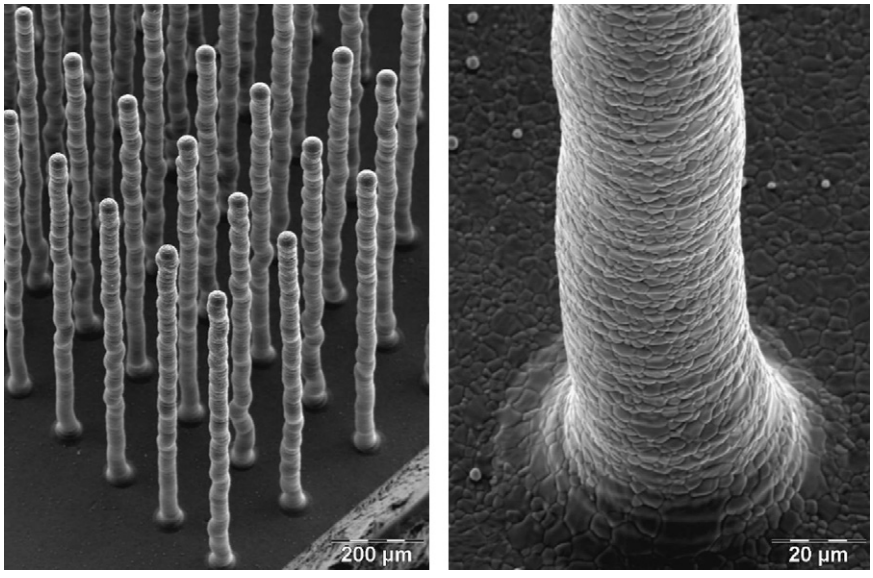

Fig. 8. Scanning electronic images of sintered TiO_2 micro-pillars, fabricated on TiO_2 green tape by simultaneously electrically driving different nozzles of the printing head (52 μm aperture) with the ink 5 (15 vol.% TiO_2 loading, high molecular weight binder, ceramic/binder ratio: 75/25, surfactant).

necessary for photocatalytic applications in the fields of water or air purification. The performances of these structures for such applications are in progress.

5. Conclusions

This paper illustrates the fabrication of different kinds of micro-pillar array structures by ink-jet printing process. So the fabrication of 1–3 piezoelectric composites and photocatalytic devices by deposition, respectively of PZT and TiO_2 suspensions was reported.

For a given final configuration of the micro-pillar array (diameter and height of pillars, space between pillars, etc.), dense micro-pillar structures can be achieved in an acceptable time by specific combination of ink-jet printing conditions (driving parameters of the printing head, time gap between two successive layers, etc.) and formulation of the ceramic suspensions (ceramic loading, nature and content of binder and surfactant, etc.). This work illustrates for two different ceramic materials, PZT and TiO_2, characterized by different density, a first approach to optimize the formulation of the suspensions and correlatively the corresponding ink-jet printing conditions to obtain (i) green micro-pillar with a high definition, compacity and good stacking of the successive layers and (ii) sintered micro-pillar with a high densification rate and mechanical strength. An experimental design could be performed to further improve the performances of these structures.

Acknowledgements

The authors would like to express their gratitude towards the European Community (the European Social Funds), the Limousin Region and the CNRS for their financial support of the present work.

References

1. Blazdell, P. F., Evans, J. R. G., Edirisinghe, M. J., Shaw, P. and Binstead, M. J., The computer aided manufacture of ceramics using multilayer jet printing. *J. Mater. Sci. Lett.*, 1995, **14**, 1562–1565.
2. Mott, M., Song, J. H. and Evans, J. R. G., Microengineering of ceramics by direct ink-jet printing. *J. Am. Ceram. Soc.*, 1999, **82**(7), 1653–1658.
3. Mott, M. and Evans, J. R. G., Zirconia/alumina functionally graded material made by ceramic ink-jet printing. *Mater. Sci. Eng. A*, 1999, **271**, 344–352.
4. Xiang, Q. F., Evans, J. R. G., Edirisinghe, M. J. and Blazdell, P. F., Solid freeforming of ceramics using a drop-on-demand jet printer. *Proc. Instn. Mech. Eng. Part B*, 1997, **211**, 211–214.
5. Reis, N., Seerden, K. A. M., Derby, B., Halloran, J. W. and Evans, J. R. G., Direct ink-jet deposition of ceramic green bodies I–II. *Mater. Res. Soc. Symp. Proc.*, 1999, **542**, 141–151.
6. Reis, N., Seerden, K. A. M., Derby, B., Halloran, J. W., Evans, J. R. G. and Grant, P. S., Ink-jet printing of wax-based alumina suspension. *J. Am. Ceram. Soc.*, 2001, **84**, 2514–2520.
7. Reis, N., Derby, B. and Ainsley, C., Freeform fabrication by controlled droplet deposition of powder filled melts. *J. Mater. Sci.*, 2002, **37**, 3155–3161.
8. Bhatti, A. R., Mott, M., Evans, J. R. G. and Edirisinghe, M. J., PZT pillars for 1–3 composites prepared by ink-jet printing. *J. Mater. Sci. Lett.*, 2001, **20**, 1245–1248.
9. Moheb, M. M. and Evans, J. R. G., A drop-on-demand ink-jet printer for combinatorial libraries and functionally graded ceramics. *J. Comb. Chem.*, 2002, **4**, 267–274.
10. Teng, W. D. and Edirisinghe, M. J., Development of continuous direct ink jet printing of ceramics. *Br. Ceram. Trans.*, 1998, **97**(4), 169–173.
11. Zhao, X., Evans, J. R. G., Edirisinghe, M. J. and Song, J. H., Ink-jet printing of ceramic pillar arrays. *J. Mater. Sci.*, 2002, **37**, 1987–1992.
12. Bertsch, A., Microstéréolithographie par masquage dynamique. Thèse de doctorat. Institut National Polytechnique de Lorraine, France, 1996.
13. Hinczewski, C., Corbel, S. and Chartier, T., Ceramic suspensions suitable for stereolithography. *J. Eur. Ceram. Soc.*, 1998, **18**, 583.
14. Doreau, F., Chaput, C. and Chartier, T., Stereolithography for manufacturing ceramic parts. *Adv. Eng. Mater.*, 2000, **2**(8), 493.
15. Hinczewski, C., Corbel, S. and Chartier, T., Stereolithography for the fabrication of ceramic three-dimensional parts. *Rapid Prototyping J.*, 1998, **4**(3), 104.
16. Chartier, T., Chaput, C., Doreau, F. and Loiseau, M., Stereolithography of structural complex ceramic parts. *J. Mater. Sci.*, 2002, **37**, 3141–3147.
17. Song, J. H., Development of metal–polymer composites for fused deposition modelling. In *Proceedings of the 7th European Conference of Rapid Prototyping and manufacturing*, 1998.
18. Lous, G. M., Fabrication of piezoelectric ceramic/polymer composite transducers using fused deposition of ceramics. *J. Am. Ceram. Soc.*, 2000, **83-1**, 124–128.
19. Tolochko, M. K., Fabrication of micromechanical component by laser sintering of fine powders. In *Proceedings of the 10th European Conference on Rapid Prototyping and Manufacturing*, 2001.
20. Zoltan, S. I. Pulsed droplet ejecting system. U.S. Patent 3,683,212, 1970.
21. Lejeune, M., Noguera, R. and Chartier, T., 3D fine scale ceramic components formed by ink-jet prototyping process. *J. Eur. Ceram. Soc.*, 2005, **25**(12), 2055–2059.